

Potential effect of tropospheric polar vortex and large-scale atmospheric circulation on extreme winter temperature over Iraq (1–15 February 2020 case study)

Khamis Daham Muslih¹, Ahmad Majid Abbas²

¹Department of Geography & GIS, College of Arts, University of Baghdad, Iraq

²Department of Geography, College of Arts, Al-Iraqia University, Iraq

*Correspondence e-mail: khamies76@coart.uobaghdad.edu.iq

 <https://orcid.org/0000-0003-0210-9619>

Abstract. The Middle East region is characterized by rapidly changing temperatures that could have a direct and severe impact on human beings. During the period 1st–15th February 2020, the weather in Iraq was characterized by extreme heat and cold temperature spells. This paper investigates the role of polar vortex and large-scale atmospheric circulation in the occurrence of these events. The data used are daily minimum temperatures for 12 meteorological stations, daily data of the Arctic Oscillation Index (AOI) and North Atlantic Oscillation Index (NAOI), and reanalysis data. Our results show that extreme daily temperatures were overly sensitive and responsive to variability in the magnitude and strength of the polar vortex. Teleconnection analysis revealed that the rapid variations of polar vortex that manifested as significant changes in the NAO–AO indexes were accompanied by strong meridional circulation activity within 45° to 70° N, which enhanced the chance of occurrence of extreme temperature events.

Key words:
polar vortex,
extreme weather,
planetary waves,
temperature anomaly,
teleconnections

Introduction

It is unequivocal that human actions have warmed the atmosphere, ocean and land (IPCC 2021). Global climate change has caused a significant increase in the severity and frequency of extreme weather events worldwide (Seneviratne et al. 2021). The increase in extreme weather events (e.g., sudden drops in temperature, droughts and dust storms) might directly and severely affect the economy, human health, the water sector and the environment (ESCWA United Nations Economic and Social Commission for Western 2017; Naqi et al. 2021; Hochman et al. 2022; IPCC 2023). Besides that, the Middle East region can be described as a global climate change hotspot due to temporal changes that are expected to occur

in meteorological features (Cramer et al. 2018; Zittis et al. 2022). Moreover, this region is characterized by rapidly changing temperatures, especially during winter months (Kushnir et al. 2017). Iraq, as one of the Middle Eastern countries located at an atmospheric crossroads, is directly and strongly controlled by a variety of large-scale atmospheric patterns such as the North Atlantic Oscillation (NAO) and the El Niño-Southern Oscillation (ENSO) (Muslih 2014; Al-Khalidi et al. 2018; Al-Qadi et al. 2021). Therefore, Iraq has been identified as one of the Arab regions most vulnerable to climate change (Elisha 2010). Furthermore, Iraq's vulnerability to the extreme weather events effects has been expected to increase as a result of capacity constraints and the lack of structures and mechanisms that can respond

effectively to mitigate climate change effects (Berghof Foundation and Peace Paradigms Organisation 2023). These mitigation strategies include, for example, developing resilient health and agricultural systems, optimizing water resources management using modern techniques, and utilizing smart city technology to improve infrastructure system management and optimization. The vulnerability index for Iraq is estimated, according to the ND-GAIN Vulnerability Index 2022, at around 43.6 (122 out of 187). This score means the country is highly vulnerable to climate change with an exceptionally low readiness level. The ND-GAIN country index is composed of two key dimensions of adaptation: vulnerability and preparedness. It summarizes a country's vulnerability to climate change and other global challenges, as well as its readiness to improve its resilience. The goal is to help governments and communities better prioritize investments for a more effective response to the immediate global challenges ahead (Notre Dame Global Adaptation Initiative 2022).

In the last two decades, numerous studies have been conducted on extreme weather events using several statistical and synoptic analysis techniques over the eastern Mediterranean and Middle East and their effects on society and ecosystems (e.g., Coumou and Rahmstorf 2012; MedECC 2020; Hochman et al. 2022; Zittis et al. 2022).

In Iraq, a country dominated by an arid and semi-arid climate, significant extreme weather events have been detected. Mohammed and Kadhum (2021) analyzed extreme cold temperature and precipitation events in Iraq during the period 1994–2018 and their linkage to general circulation patterns. Muslih and Błażejczyk (2017) evaluated the inter-annual variations and long-term trends of monthly temperatures at seven selected meteorological stations using the Mann–Kendall (MK) test and linear regression.

The study by Muslih and Błażejczyk (2017) suggested warming trends, which were strongest during the summer months. Salman et al. (2017) investigated temperature extremes in Iraq over the period 1965–2015. They reported that the number of hot extreme nights is getting higher at a rate of 2.92 to 10.69 days/decade. Yet, the number of chilly days is decreasing at a rate of –2.65 to –8.40 days/decade. Further studies determined the climatic and

synoptic factors responsible for the occurrence of the cold wave and snowfall in Iraq from 09/02/2020 to 13/02/2020 (e.g., Abdul Rahman 2021; Mahmoud 2021; Al-Saadi 2023). Both studies reported that this cold wave was associated with a cold polar air mass advection generated by the Siberian anticyclone at the surface and with a deep trough at the level of 500 hPa. Moreover, many other studies have also shown a significant increase in extreme temperature events in this country (e.g. Al-Timimi and Al-Khudhairy 2018; Al-Timimi et al. 2020; Al-Budeiri 2021; Mutar and Hamad 2024).

Further, with the increased frequency of mid-latitude extreme weather events, dramatic changes in the Arctic climate system appear to have occurred. The link between extremely weak (strong) polar vortex and changes in extreme weather is not well understood, especially since polar vortex variability is expected to increase in the coming decades (Cohen et al. 2014). In recent years considerable studies have analyzed the potential link between the polar vortex and weather variability at midlatitudes (e.g., Francis 2017; Screen et al. 2018; King et al. 2019; Matthias and Kretschmer 2020; Overland et al. 2020; Finke et al. 2023; Galytska et al. 2023). These researchers found that the polar vortex shifting southward is frequently linked to extreme surface weather, such as abnormally low temperatures, and to extreme snow events caused by the upper-tropospheric polar jet stream migrating equatorward.

Some studies have analyzed the relationship between the polar vortex and precipitation and winter temperature anomaly in selected countries of the Middle East (e.g., Kömüscü and Oğuz 2021; Rahimi 2021). Despite the several scientific studies concerned with the impact of large-scale atmospheric circulation patterns on Iraq's climate, no study has investigated the potential links between polar vortex and extreme temperature anomaly over Iraq. Therefore, the main objective of this paper is to quantify the role of the polar vortex in shaping the extreme winter temperature anomalies in Iraq (1–15 February 2020 as a case study). Moreover, the paper aims to explore the potential causal synoptic relationship between the Arctic climate system and extreme temperature events in Iraq. In a sense, we aim to determine the physical mechanisms through which the variations in the strength of stratospheric polar vortex affect winter temperature anomalies over Iraq.

Materials and methods

Our study focuses on the period from the 1st to the 15th of February 2020; we use daily minimum temperature data for twelve meteorological stations that provide data continuously. These stations were strategically located across the study area, providing comprehensive coverage from 1985 to 2020, (Table 1, Fig. 1). All recorded temperature data was obtained from the Iraqi Meteorological Organization. Here, we elaborated anomalies of minimum temperature data in selected metrological stations over Iraq, calculated relative to the climatological mean 1985–2020. That is to say, the daily minimum temperature on a specific day was subtracted from the multi-year mean of that day to determine anomalies.

The synoptic analysis is based on reanalysis data derived from the National Center for Environmental Prediction (NCEP) and the National Center for Atmospheric Research (NCAR) with $2.5^\circ \times 2.5^\circ$ spatial resolution (Kalnay et al. 1996).

To achieve the goal of this study, five meteorological elements were investigated: geopotential height at 850 hPa, 500 hPa and 100 hPa levels, Sea Level Pressure (SLP), and wind speed (m/s) at 250 hPa level. Only geopotential height at 250 hPa was selected for wind speed, since the jet stream appears at this level and determines polar front position in the surface, which is the prominent signature of Middle East climate fluctuations in winter. The composites tool from the

Earth System Research Laboratory of NOAA was used to derive composite maps for the Middle East and adjacent areas. The daily minimum temperature within 50° – 90° N at the 100 hPa level was also used in our analysis. All these data were obtained from the NOAA Physical Sciences Laboratory. Daily values for Arctic Oscillation Index (AOI) data (Thompson and Wallace 1998) and North Atlantic Oscillation (NAO) index data were supplied by the Climate Prediction Center (CPC) of the National Centers for Environmental Prediction (NCEP) (Hurrell 1995).

Following previous studies (e.g., Polvani and Waugh 2004; Matthias and Kretschmer 2020; Zhang et al. 2021b), to assess the strength of the polar vortex, the zonal-mean zonal wind at 60° N is calculated. One commonly used method to measure the upward-propagating planetary wave activity is the meridional eddy heat flux at 100 hPa. Many studies have found that variations in the eddy heat flux at 100 hPa determine the stratospheric interannual variability (e.g., Zhang et al. 2021b). Thus, the meridional eddy heat flux at 100 hPa averaged within 45° – 75° N was used in this study.

The Pearson correlation coefficient has been used to better understand and statistically accurately assess the relationship between parameters describing polar vortex intensity and daily air temperature. The Pearson correlation test has been standard as one of the most common methods for assessing reliance between two variables using the following equation (Rodgers and Nicewander 1988):

Table 1. Details of the selected meteorological stations used in this study

Station	Latitude (N)	Longitude (E)	Altitude (m a.s.l.)
Sulaimaniya	35°32'	45°27'	843.0
Rutba	33°02'	40°17'	615.5
Kirkuk	35°28'	44°24'	330.8
Nukhaib	32°02'	42°15'	305.0
Mosul	36°19'	43°09'	222.6
Khanaqin	34°35'	45°38'	175.0
Baghdad	33°29'	44°24'	34.1
Najaf	31°59'	44°19'	32.0
Diwaniya	31°59'	44°59'	20.4
Hai	32°10'	46°03'	17.0
Nasiriya	31°01'	46°14'	3.0
Basrah	30°34'	47°47'	2.4

Source: authors' own elaboration

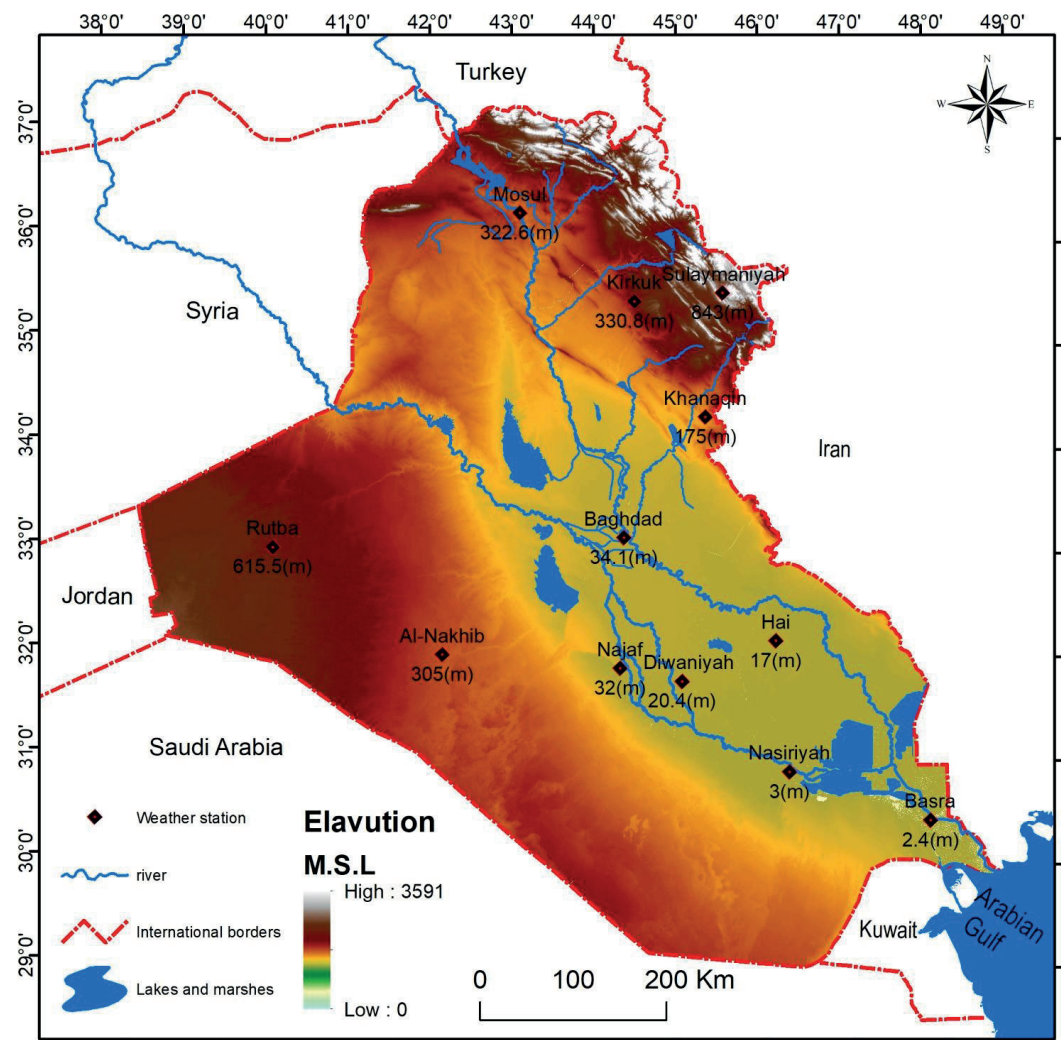


Fig. 1. Topographic map of Iraq with spatial distribution of meteorological stations used in the paper
Source: authors' own elaboration

Results and discussion

$$r_{xy,j} = \frac{i=\sum_{1971}^{2016} (x_{i,j} - \bar{x}_j)(y_{i,j} - \bar{y}_j)}{(n-1)S_{x,j}S_{y,j}}$$

Where: $r_{xy,j}$ = correlation coefficient; $x_{i,j}$ and $y_{i,j}$ = the daily air temperature and the parameters describing polar vortex intensity over the study period; $S_{x,j}$ and $S_{y,j}$ = the standard deviation in the parameters describing polar vortex intensity and daily air temperature, respectively; and n = the number of data cases. A correlation coefficient was considered statistically significant when the null hypothesis was exceeded with a probability level of 95%.

Temperature variability, 1st–15th February 2020

February 2020 was different from other Februaries of the entire study period (1985–2020) (Fig. 2). At the start of the month, the temperature was around its average in all stations. Gradually, the temperature started to rise, until it reached its highest temperature anomaly values on the 6th of February: these were 3.9 °C in Rutba in the west of Iraq and 3.9 °C at Sulaimaniya station at the northeastern tip of Iraq.

Other stations registered the highest minimum temperature on the 7th of February. At Nukhaib station it occurred one day later (8th of February). The temperature anomalies at most stations were greater than 5°C, with the highest anomaly of 6.9°C recorded at the Basrah station in southern Iraq (Fig. 3). As shown in Figure 2, after February 8th, the temperature dropped exceptionally at all stations included in this study.

The lowest minimum temperatures in the study area were recorded on 11th February for 50% of stations across the west and north of the country, including at Mosul, Sulaimaniya, Kirkuk, Khanaqin, Rutba and Nukhaib stations, with minimum

temperature anomalies of -6.1, -10, -7.2, -7.6, -10.0 and -8.1 °C, respectively, “breaking the record”. Another 50% of stations in central and southern Iraq (Baghdad, Hai, Najaf, Diwaniya, Nasiriya and Basrah) registered absolute minimum temperature anomalies of -8.5, -8.0, -7.7, -8.0, -7.8 and -7.8 °C, respectively. Owing to the very low temperature reached within the continental polar air masses associated with the Siberian anticyclone, very heavy snowfall in north Iraq lasted continuously for three days (10–12 February) while in the center and west of Iraq snowfall accumulated only on 11th of February (Abdul Rahman 2021).

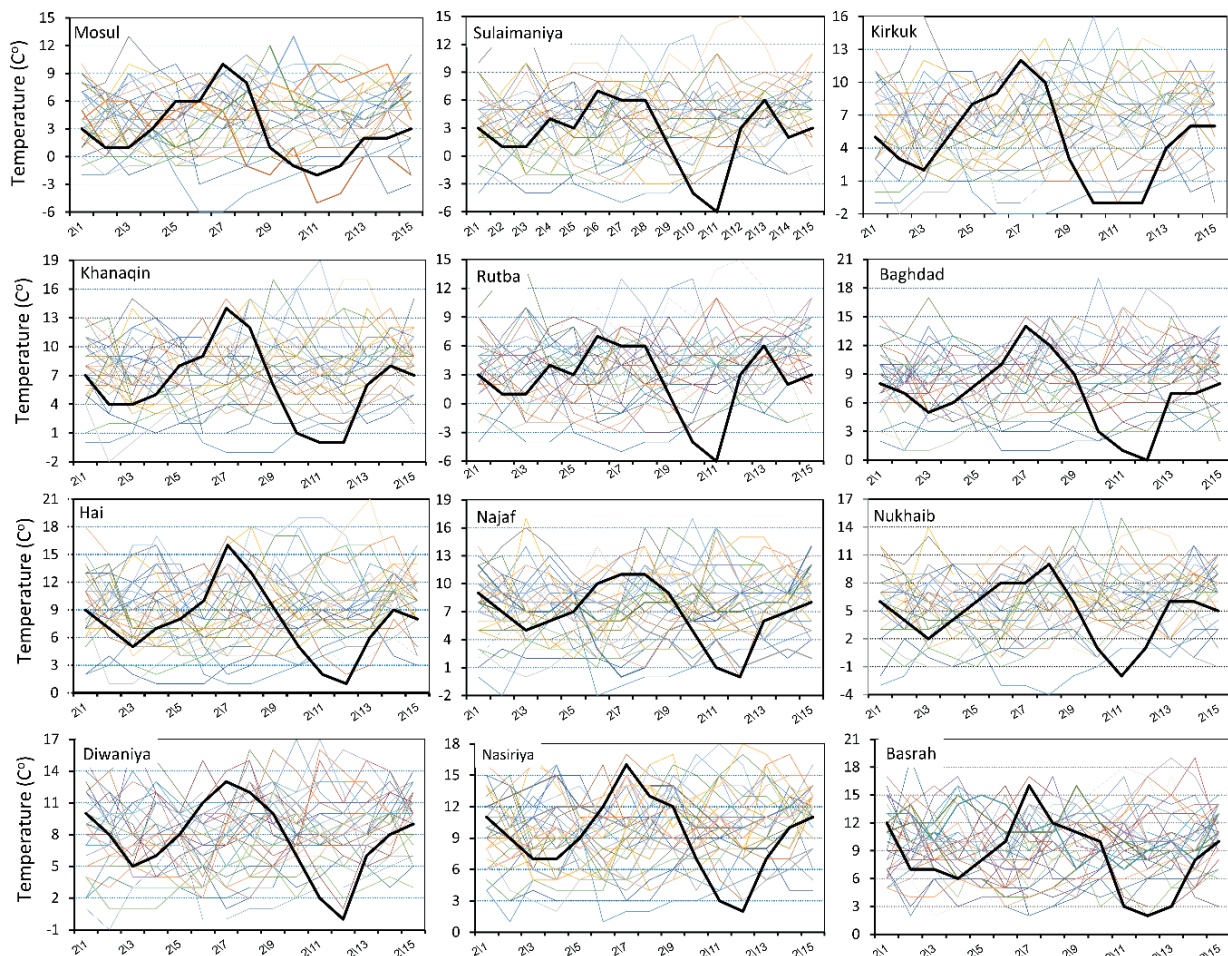


Fig. 2. 1–15 February daily minimum air temperature for selected meteorological stations over the period 1985–2020; black lines are daily mean temperature during the period February 1–15, 2020. The daily mean temperature for each year from 1985 to 2020 is represented by the individual colored lines.

Source: unpublished data from Iraqi Meteorological Organization and Seismology

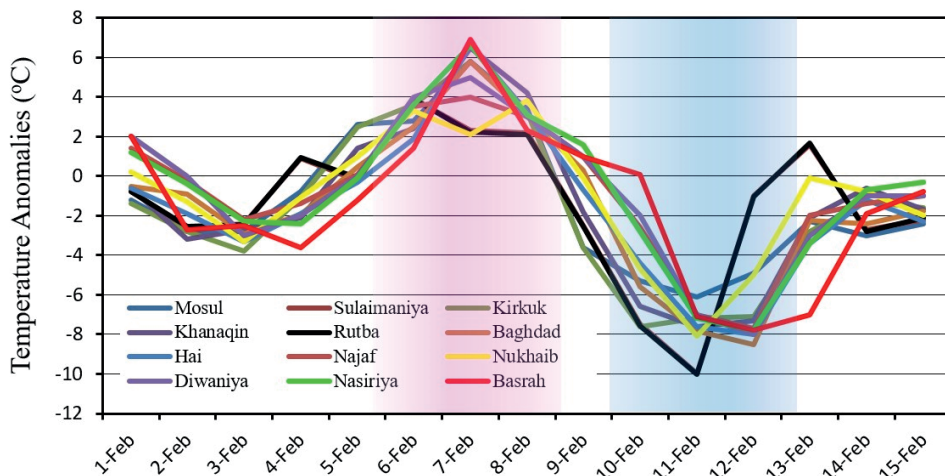


Fig. 3. February 1–15, 2020 daily minimum air temperature anomalies for selected meteorological stations relative to the climatology average over 1985–2020

Source: unpublished data from Iraqi Meteorological Organization and Seismology

Synoptic evolution

Synoptic environment prior to the formation of heat wave

This section discusses the synoptic development associated with two contradictory extreme events during the first two weeks of February 2020 (February 1–15). The first was the abnormal heat wave, which reached its peak on February 6 and 7, with a temperature anomaly ranging from 3.8°C at the Nukhaib station in western Iraq to 6.9°C at the Basra station, located in the far south of Iraq. On 3–5 February 2020, the lower level of the atmosphere was dominated by a subtropical high with a west–east axis extending from the tropical Atlantic Ocean over North Africa and reaching the central pressure of 1023 hPa. This high-pressure configuration extended over all of Iraq from the north to the south (Fig. 4). The vertical structure of this system was deep enough to appear on the maps of 850 hPa geopotential height.

The geopotential map at 500 hPa level shows small amplitude waves over all eastern Mediterranean regions “including Iraq”, which means less interference of both tropical and polar air masses. The synchronous 250 hPa wind speed field shows that the core of the subtropical jet stream is lying over the Arabian Peninsula, south of Iraq, with a pronounced horizontal wind shear on the northward flank of the jet (Fig. 4). The simultaneous

synoptic conditions contributed to the prevalence of atmospheric stability over the entire Eastern Mediterranean region. Nevertheless, the anticyclone over the border between Iraq and Iran visible on the 3–5 February maps is induced by the upper-level convergence which is usually present in the left rear (LR) region of the jet stream (jet streak).

Heat wave: second stage of development

On February 6 and 7, surface temperature anomalies showed a clear increase compared to the climatological average from the period 1985–2020 (Fig. 5). Synoptic conditions during those days are represented in Figure 5. The study area is still dominated by a deep subtropical high with axis extended towards the southeast, so that it has a southeast–northwest axis covering all the Arabian Peninsula and the eastern Mediterranean region, centered over Iran and eastern Iraq enclosing an anticyclone, with a central surface pressure value of up to 1021 hPa. This high-pressure system is also visible at the 850 hPa level. It can be seen that, at 500 hPa, ridges extended over the eastern Mediterranean region with a north–south axis direction.

The geopotential map at 250 hPa shows a blocking pattern, with high values over Iran and Iraq, which splits the jet stream into two branches; the northern one, going northeasterly over Turkey and the southern part situated over the Arabian Peninsula. This atmospheric circulation within the surface and

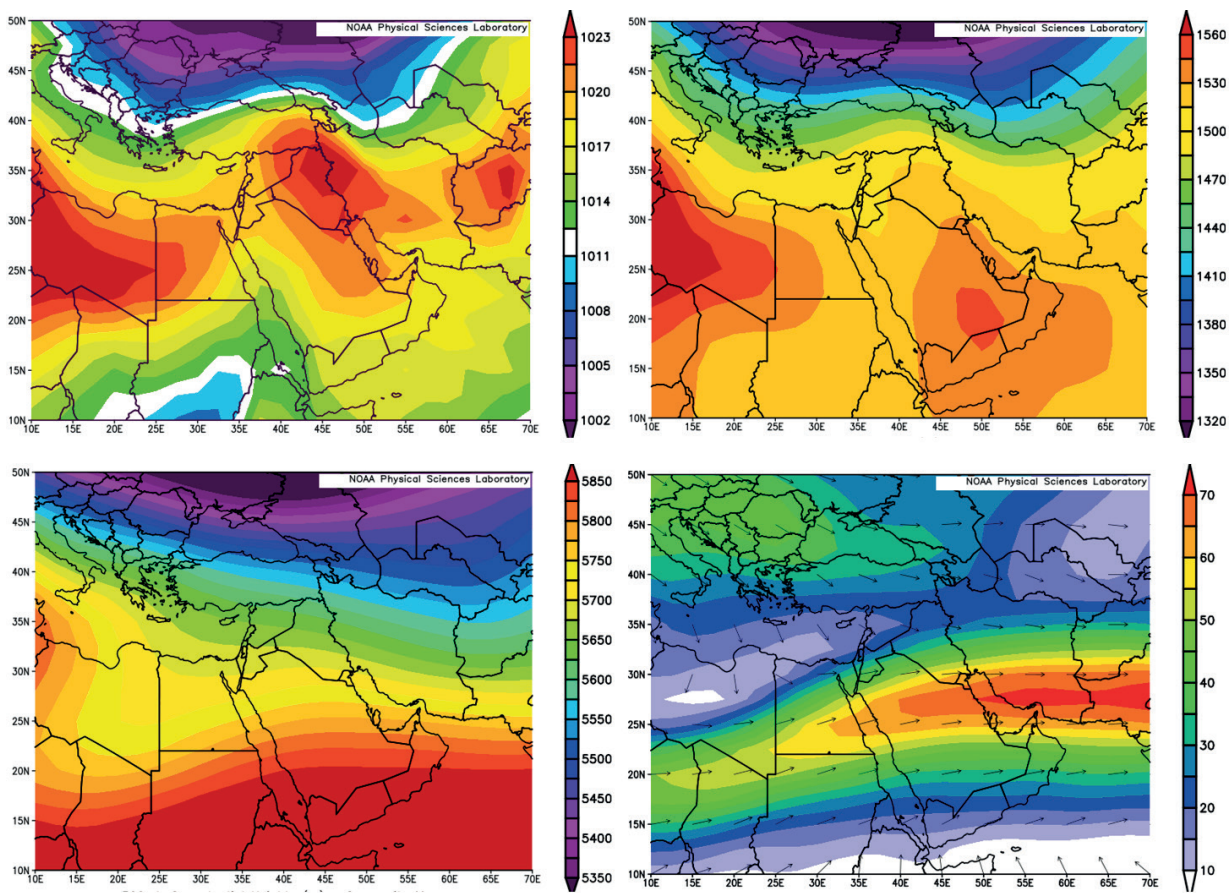


Fig. 4. Synoptic patterns for February 3–5, 2020, 00 UTC. Upper panels: Mean sea level pressure (left) and geopotential height at 850 hPa (right). Lower panels: Geopotential height at 500 hPa (lift) and wind speed for the Middle East region at level 250 hPa (right)

Source: data provided by NOAA Physical Sciences Laboratory 2021

upper levels contributed to the transport of warm and dry sub-tropical masses from the Arabian Peninsula towards Iraq, causing unusually high temperatures at that time of year over the study area.

Synoptic conditions during cold wave occurrence

In the following days, rapid and sudden evolutions in synoptic conditions at all atmospheric levels are observed. On February 8 and 9, temperatures returned to the climatological daily mean with a state of atmospheric stability. Subsequently, the second anomalous weather event began, represented by a rapid drop in temperatures for all parts of Iraq. The negative temperature anomaly reached its nadir on February 11 and 12, as we have shown in detail

(section 3.1). Analyzing circulation patterns of this cold event, we find the following (Fig. 6):

On 10 February: The wind speed field maps at 250 hPa show the blocking anticyclone shifting eastwards, giving way to the control of the polar jet stream and affecting Iraq, where the center of the jet stream was passing over Kuwait and southern Iraq. At that time, the upper westerlies started meandering and led to the extension of a deep trough with a northeastern–southwestern direction at mid-tropospheric level. However, the center of the low at 500 hPa level, is located over Turkey. Therefore, its effect on reducing temperature on this day was more evident in the northeastern parts of Iraq, as is the case at the Sulaimaniya and Kirkuk stations (Fig. 3). The lower-level synoptic conditions were very similar to the upper level's circulation patterns in terms of nature and extension. On the surface, there was

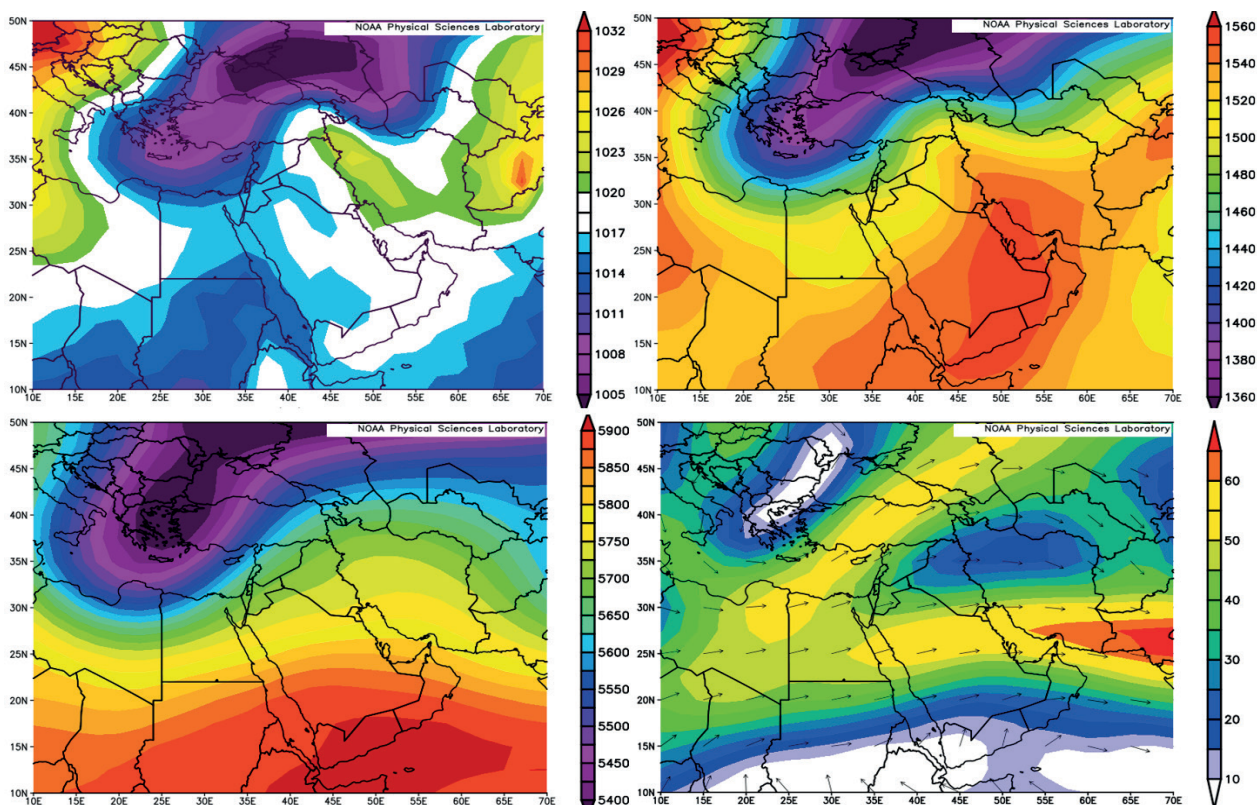


Fig. 5. Synoptic patterns for February 6–7, 2020, 00 UTC. Upper panels: Mean sea level pressure (left) and geopotential height at 850 hPa (right). Lower panels: Geopotential height at 500 hPa (left) and wind speed for the Middle East region and adjacent areas (m/s) at level 250 hPa (right)

Source: data provided by NOAA Physical Sciences Laboratory 2021

an extension of the Siberian anticyclone over Turkey towards the southwest over the Mediterranean Sea, and it was merged with the subtropical high centered over North Africa, the Mediterranean Sea and southern Europe. This merger was not maintained in the layers, as it did not appear on the weather maps at the 850 hPa level. At that time, a vast ridge from the Siberian high spreading westward over Iraq affected only the north and northeast of Iraq, as shown above in Fig. 6.

Figure 6 also depicts the circulation pattern of 11 February 2020. The elevated waviness of the upper atmosphere has increased, and the westerlies become more meandered, as Iraq has come directly under the influence of the curvature of the cold polar jet stream at 250 hPa level. At the 500 hPa level, the westerlies turn southwards, affecting all parts of Iraq and associated with the evolution of a well developed trough with a northeast–southwest axis. This pattern of extension of the upper system created an optimal atmospheric condition for very cold continental polar

masses to break out towards Iraq. On the surface, a massive ridge of Siberian anticyclone extended over Iraq with an east–west axis, enclosing a deep anticyclone over southern Turkey and reaching the central pressure of 1035 hPa (Fig. 6).

The high pressure was represented on the surface and 850 hPa levels. The prevailing synoptic condition on 11 February was responsible for the dominance of the extremely cold event over Iraq. On the surface, the Siberian high dominated, and in the middle atmosphere, there is a deep trough associated with a polar jet stream at 250 hPa level causing very cold masses to penetrate towards Iraq. Additionally, heavy snow had fallen on the early morning of February 11 on most of northern and central-western Iraq. This is exceptional if one considers the domination of the Siberian high, which creates a stable atmospheric condition in the lower atmosphere. Our explanation for this distinctive case is that, despite the Siberian high's domination on the surface, the presence of the center of the upper trough at 500 hPa contributed

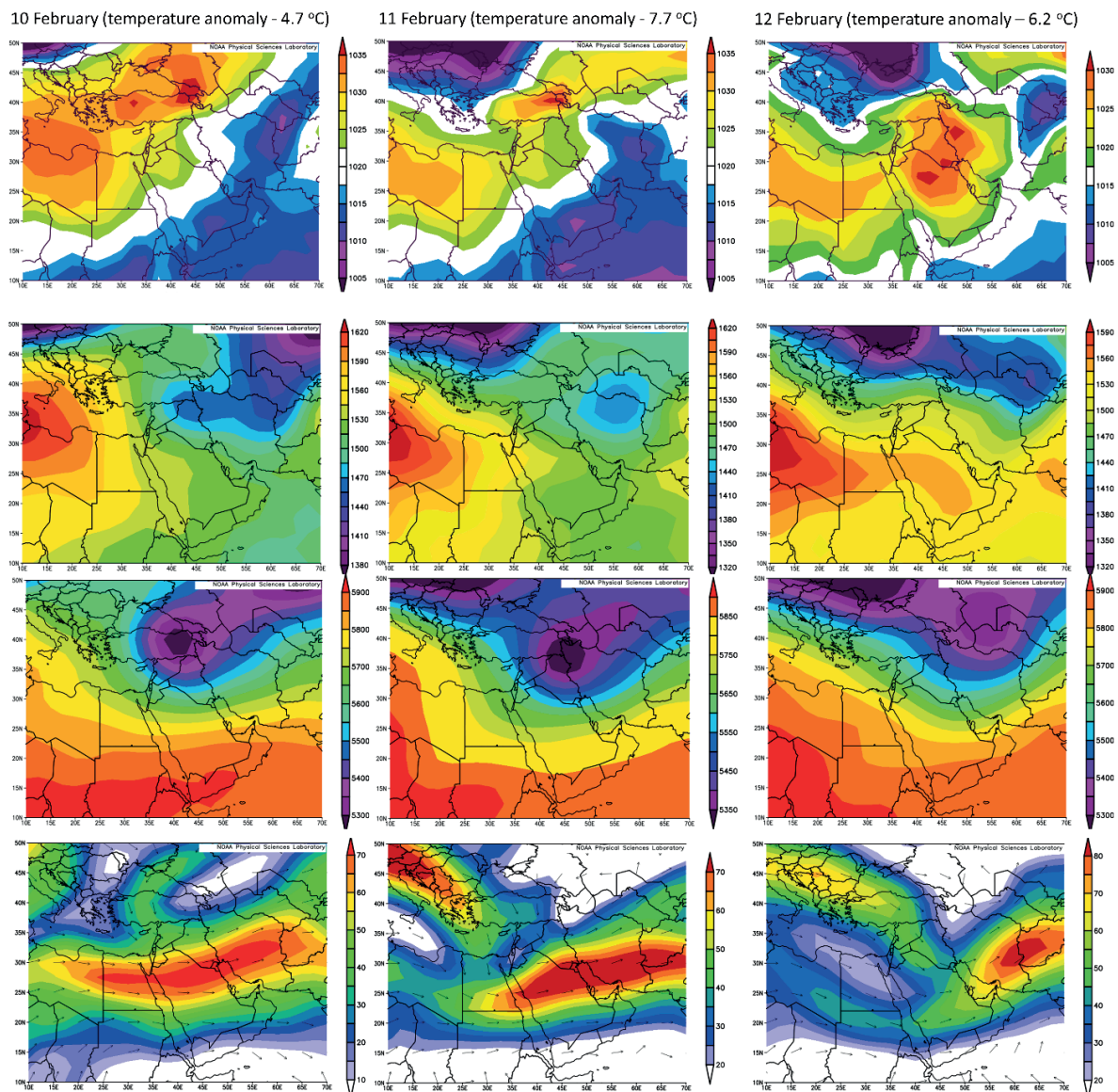


Fig. 6. Synoptic patterns for February 10–12, 2020, 00 UTC (from left to right respectively). Mean sea level pressure (hPa) (Upper panels); Geopotential height at 850 hPa (second row panels, from top); Geopotential height at 500 hPa (third row panels from top); and wind speed for the Middle East and adjacent areas (m/s) at level 250 hPa (bottom panels)

Source: data provided by NOAA Physical Sciences Laboratory 2021

to the ascending motions in the upper layers of the atmosphere. Therefore, air rose from the surface, which, due to its cold temperature, quickly reached its dew point, resulting in snowfall that day.

On February 12, the upper westerlies began to slow down over Iraq and move northwards, accompanied by northwards and northeastwards movement of the upper cyclone center at the 500 hPa level, leading to less chance of very cold air masses reaching the study area. As the pressure systems at upper levels moved, on the surface the

Siberian high began simultaneously to retreat from Iraq towards the northeast. This retreat allowed the subtropical high to move towards the study area from the west. The subtropical high established an independent center of high pressure with a southwestern–northeastern axis extending from the Arabian Peninsula to northern Iran, allowing the warm dry tropical masses to progress towards the Eastern Mediterranean region, and ending the exceptional cold event.

The polar vortex

The polar vortex can be defined as the large area of chilly air and low pressure that surrounds each pole (Waugh et al. 2017). In the Earth's atmosphere, there are two polar vortices that differ in terms of dynamics, structure, seasonality and impacts on surface weather (AMS 2015). The first is a tropospheric vortex that is commonly defined by geopotential height contours lying in the core of the westerlies. The equatorward edge of the tropospheric vortex is around 40° to 50° latitude, and it exists throughout the year (Angell 2006; Waugh et al. 2017). The other is the stratospheric polar vortex, which is defined by the small geopotential height area encircled by strong westerlies at about 15 km to 50 km altitude, maximizing at 60° and edge positioned around 50°

latitude. The stratospheric polar vortex exists from autumn to spring and completely disappears during summer (Schoeberl and Hartmann 1991).

Many recent studies have focused on the polar region, proposing that the stratospheric polar vortex variability can directly affect mid-latitude extreme weather events (e.g., Baldwin and Dunkerton 2001; Francis and Vavrus 2012; Cohen et al. 2014; King et al. 2019). In this section, we investigate the influence of the polar vortex on extreme temperature events during the first two weeks of February 2020 in Iraq, a Middle Eastern nation subject to mid-latitude climatic dynamics.

The winter of 2019/20 was marked by an exceptionally strong and persistent stratospheric north-hemisphere polar vortex, accompanied

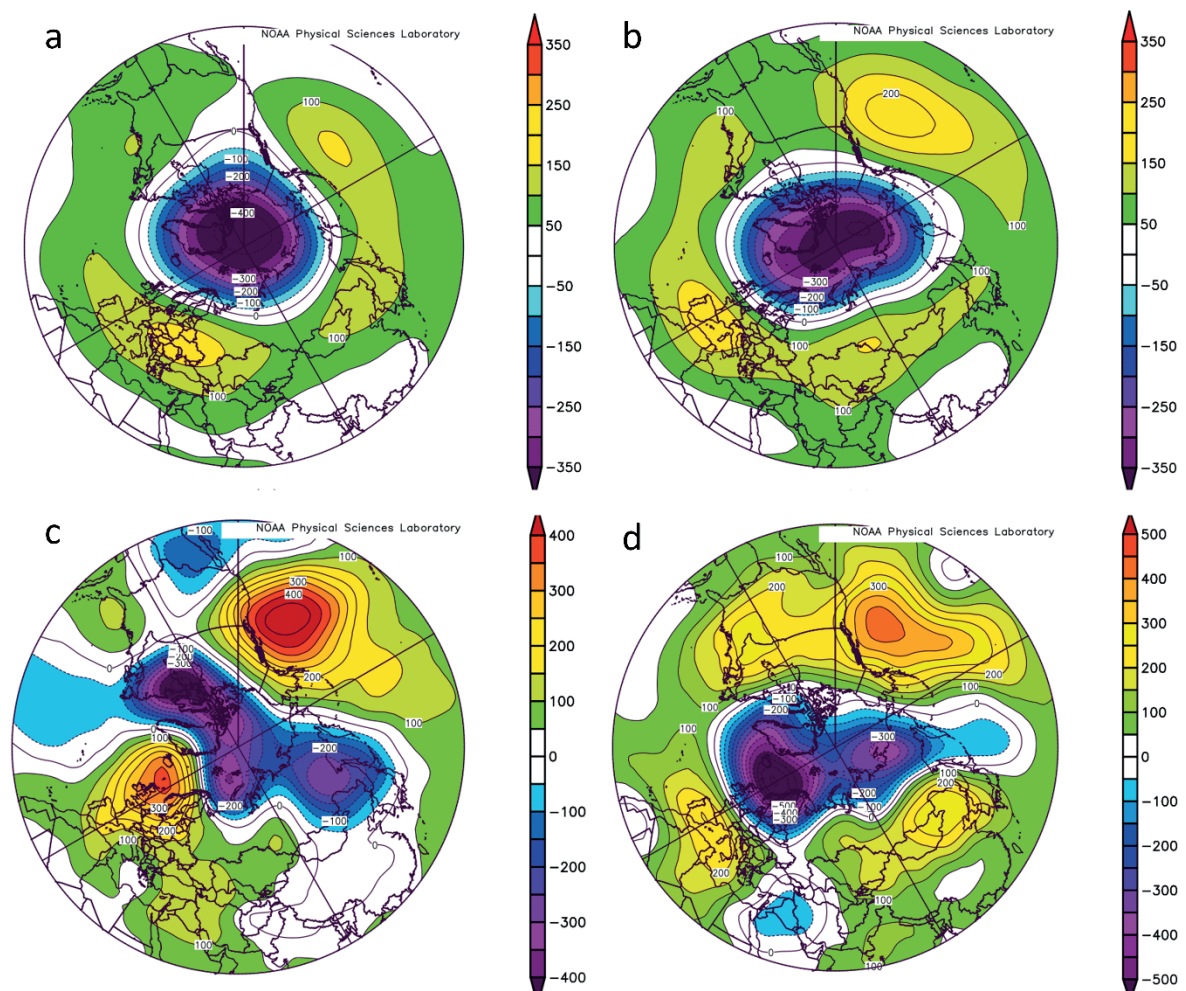


Fig. 7. 100 hPa geopotential heights anomalies relative to 1981–2010 base period for: from January 1 to March 31, 2020 (a) and February 2020 (b). Lower panels: February 6 2020 (c) and February 11 2020 (d)
Source: data provided by NOAA Physical Sciences Laboratory 2021

by poleward-shifted extratropical cyclone tracks, which led to a remarkably warm and quiet winter across NH mid-latitudes (Lee et al. 2020; NOAA 2020; Zhang et al. 2021a, b). It has been recognized as the strongest on record at 10 and 100 hPa since 1979/80 (Lawrence et al. 2020). Figure 7A shows the 100 hPa geopotential heights anomaly over January through March 2020. An outstanding feature in this figure is that the high strength of the polar vortex lasted over most of January to March. In this map, only one negative polar vortex anomaly center was located exactly over the North Pole and was associated with the polar vortex having a lower-than-climatological-mean minimum temperature (Fig. 8C).

The exceptional polar vortex during the 2020 winter (January to March) was surrounded by very strong westerly winds at 60°N (Fig. 8B). The same figure also shows that the zonal-mean zonal winds were speedier than the climatological mean (the blue line Fig 8B). On the other hand, more than 70% of the daily mean of eddy heat flux ($\text{K}\cdot\text{m}^2\cdot\text{s}^{-1}$) over 45°–75° N during the period (January to March 2020) were smaller than climatological mean for the period 1978–2021. So, the upward planetary wave activity during this winter was low compared with other winters. As is known, less propagation of Rossby waves usually results in a strong polar vortex, and vice versa (Zhang et al. 2021b) (Fig. 7A). Moreover, during the winter and spring of 2019/20, the lesser activity of planetary waves was considered the main reason for the strong and persistent polar vortex (Zhang et al. 2021).

The 100 hPa geopotential heights anomaly for February 2020 is shown in Figure 7B. It is obvious that the polar vortex was still strong and had one center located over the North Pole, associated by extraordinarily strong zonal wind at 60° N latitude (Fig. 8B). However, the polar vortex started to take on an elliptical shape during this month.

The most notable change in the polar vortex during the winter of 2019/20 occurred in the first half of February 2020. The variation in polar vortex during 1st to 15th February 2020 led to significant variation in daily temperature over Iraq. Daily minimum temperatures were correlated with some parameters describing polar vortex intensity (see Materials and methods section) at twelve stations during the period (1–15 February 2020). Moreover, Table 2 suggests that the polar vortex influences daily temperature in Iraq, and this influence can vary significantly from one parameter to another. For example, a significant

negative correlation between daily temperature and zonal-mean zonal wind at 60° N at $\geq 95\%$ confidence level was found for 75% of stations included in this study. A significant positive correlation statistic was obtained with daily minimum temperature within 50°–90° N for some stations, particularly for the north and northeast of Iraq.

On the other hand, Table 2 demonstrates a lack of significant negative correlation between daily minimum temperature over Iraq and daily mean eddy heat flux over 45°–75° N. Again, the heights correlation coefficients related to the zonal-mean zonal wind at 60°N. That does not mean that there is no correlation with other polar vortex parameters, but the low correlations may partly reflect a less direct relationship with local climatic factors.

On February 6 (Fig. 7C), the polar vortex divided into two cells: the larger and stronger intensity center was located over North America west of the Greenland Sea; the second was located over Eastern Eurasia at 60° N latitude. The displaced polar vortexes were surrounded by a sudden reduction in speed of the zonal-mean zonal wind at 60°N compared to its speed over the previous days, as shown in Fig. 8B. Additionally, Figure 8A also reveals an abrupt increase in the meridional eddy heat flux within 45°–75° N compared with the climatology of 1978–2021. This increase in the meridional eddy heat flux indicated an upward propagation of planetary waves that reinforced the events of the first half of February. An upward propagation of Rossby waves increased poleward heat transfer in the northeast Atlantic sector.

The upward spread of planetary waves led to an increase of the daily minimum temperature within 50°–90°N at 100 hPa during this event that approached the climatology of 1978–2021, as shown in Figure 8C.

The regional intensification of the displaced polar vortex and their descendant effects on mid-latitude waves are shown in Figure 7. The center of the polar vortex located over North America was large enough to direct northward the polar jet stream over the north-eastern part of the Atlantic and western Europe, associated with a large mass of warm air moving upward toward the North Atlantic and eastern Mediterranean region, including Iraq (Fig. 9C and E). The warm tropical mass air caused a rapid increase in air temperature over Iraq on 6th and 7th of February 2020. In contrast, Figure 9D illustrates that the cold polar air penetrates southward

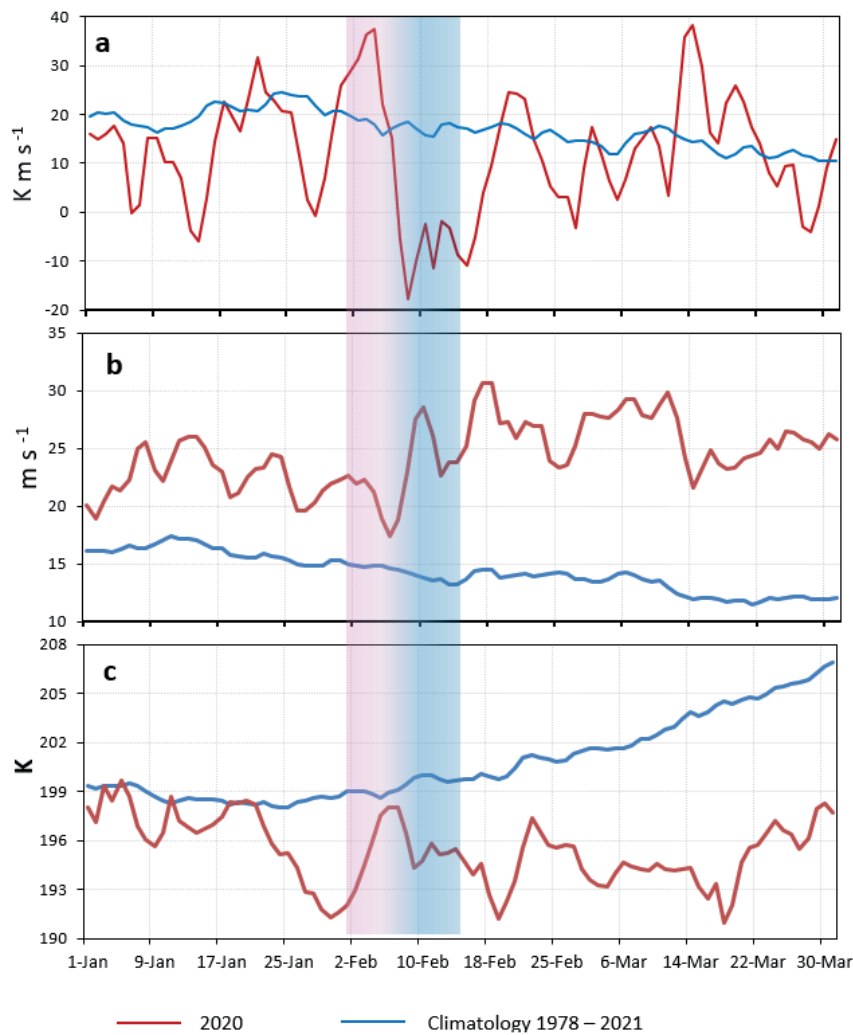


Fig. 8. 100-hpa variations of (a) the daily mean eddy heat flux over 45° – 75° N ($\text{K} \cdot \text{m} \cdot \text{s}^{-1}$), (b) zonal-mean zonal wind at 60° N (m s^{-1}), and (c) daily minimum temperature within 50° – 90° N (K)

Source: data provided by NOAA Physical Sciences Laboratory 2021

Link to NAOI and AOI

across central European regions until it reaches the Mediterranean Sea. Subsequently, the polar vortex (which was over North America) started to move toward the east, then centered over the North Atlantic east Greenland on February 11, as shown in Figure 9D. This caused a massive chilly air flow southward to the Middle East region shown on maps of 500 hPa (Fig. 9D and 9F), which led to extreme cold across all this region including Iraq with temperature anomalies reaching more than -10°C , as explained in the section headed “Temperature variability in the period 1st–15th February 2020”.

Correlations between geopotential heights on a certain pressure surface at widely separated sites on Earth are referred to as “teleconnections”. The main benefit of studying teleconnections is to identify and document recurring spatial patterns with durations ranging from a few days to a month or longer that may be signs of standing oscillations in the planetary waves (Wallace and Gutzler 1981). Therefore, NAOI and AOI are two of the most studied teleconnection patterns in the Northern Hemisphere.

Shifts in the NAO–AO indices affect temperature and precipitation in the mid-latitude zone of the

Table 2. Correlation between parameters describing polar vortex intensity and daily air temperature at twelve stations during the period (February 1–15, 2020). Significant correlations at <0.05 are shown in bold.

Station	Daily mean eddy heat flux over 45°–75° N	Zonal-mean zonal wind at 60° N	Daily minimum temperature within 50°–90° N
Mosul	- 0.02	- 0.68	0.59
Sulaimaniya	0.09	- 0.68	0.36
Kirkuk	- 0.03	- 0.66	0.55
Khanaqin	- 0.13	- 0.53	0.46
Rutba	0.09	- 0.68	0.36
Baghdad	- 0.07	- 0.45	0.34
Hai	- 0.13	- 0.41	0.36
Najaf	- 0.02	- 0.34	0.19
Nukhaib	- 0.09	- 0.47	0.32
Diwaniya	- 0.12	- 0.32	0.21
Nasiriyah	- 0.12	- 0.32	0.23
Basrah	- 0.20	- 0.17	0.15

Northern Hemisphere (Zhang et al. 2020). Many studies have found that the positive (negative) phases of NAO–AO indices are typically associated with stronger and colder (weaker and warmer) stratospheric polar vortex. This results in smaller (larger) upward-propagating planetary waves and, eventually, lower (higher) frequencies of extreme weather events (e.g., Kuroda 2002; Baldwin et al. 2003; Zhang et al. 2021b). The regression line (Fig. 10B and C) suggests a negative correlation ($r=-0.21$ and -0.06) between the daily winter temperature over the Iraq and AOI and NAOI, respectively, significant at the 95% probability level, where the AO and NAO indexes explain 21–41% of Iraq's temperature variability during wintertime. However, links among NAO or AO indexes and rainfall and temperature in the Iraq have been examined by many recent studies (e.g., Muslih 2014; Khidher and Pilesjö 2015; Mohammed and Kadhum 2021; Hassan and Al-Asadi 2023). These research papers have also shown a strong and immediate response of the climate condition in the Middle East region “including Iraq” to changes in Arctic–Atlantic weather systems. Figure 10A clearly illustrates that positive NAO–AO indexes for the entire three winter months of January–March (2020) constituted around 84% for NAOI and 97% for AOI. Figure 10 also shows that temperature correlates more strongly with AO than with NAO. Perhaps this

is due to the worldwide impact of NO, unlike the NAO oscillation, which has a lesser influence than the first. According to studies including Thompson and Wallace (1998), the NAO represents the local expression of the AO, a worldwide pattern. This AO results from the interaction of tropospheric circulation with the stratospheric polar vortex.

A negative phase of NAO–AO indexes was observed before onset of both extreme weather events, specifically at the end of January. With approaching of the onset of the first extreme high temperature, the NAO–AO indexes suddenly changes over a short period from nearly -0.47 and -0.08 on 28th January to around $+1.63$ and $+3.84$ by 7th of February, respectively, “accompanied by the highest temperature anomaly during our case study period (Fig. 10A and Fig 3)”. One more abrupt change in the NAO index occurred a few days later, when the NAO index dropped to 0.783 by February 11, associated with lowest temperature anomaly during case study period (ranging from -6.1°C to -10°C) (Fig. 10.A and Fig. 3).

Numerous scientific studies have been confirming that such these huge variables of the NAO–AO indexes by about 2.1 for NAOI and 3.92 for AOI are significant and represent a noticeable circulation pattern change over the Northern Hemisphere (e.g., Cellitti et al. 2006).

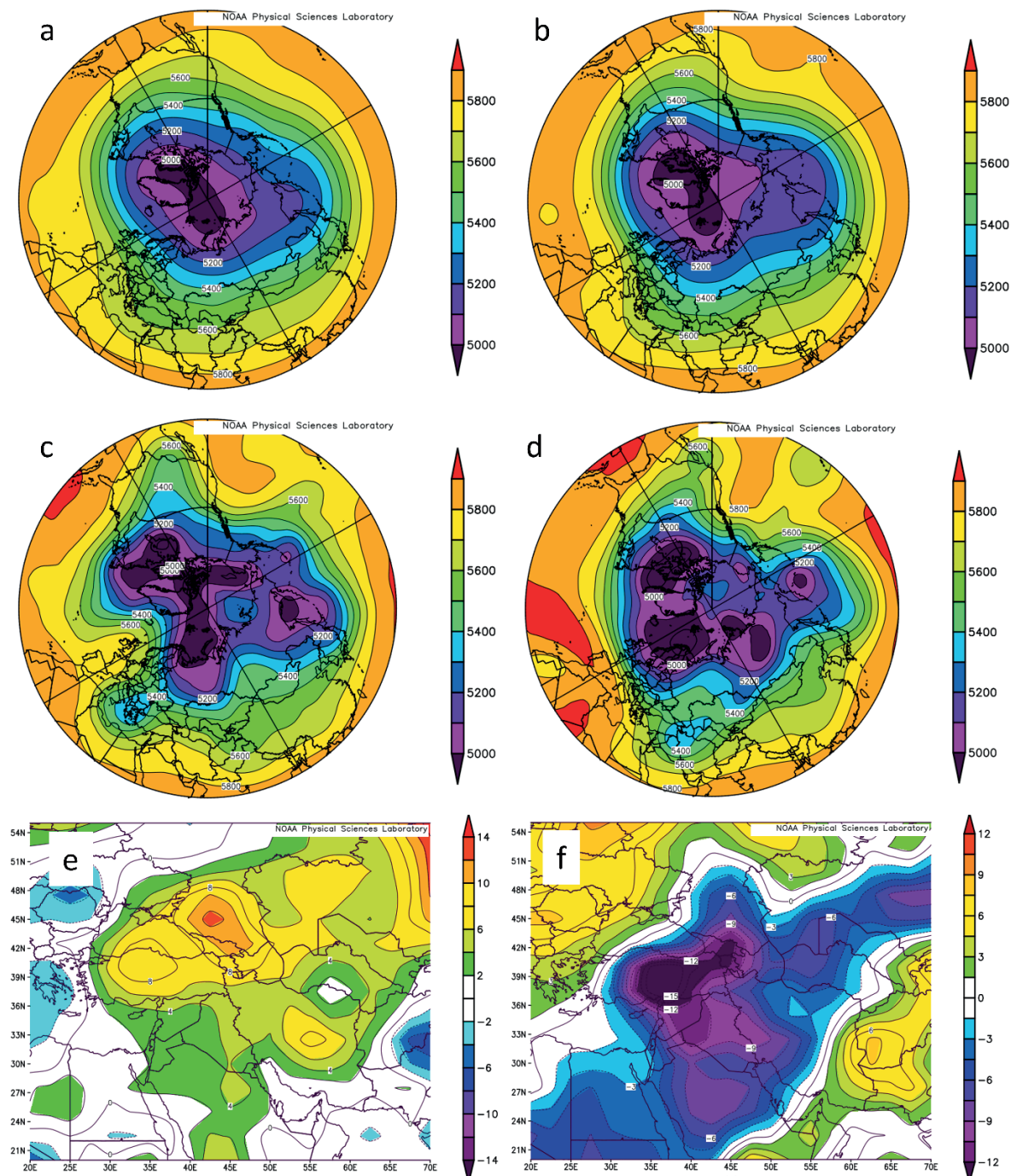


Fig. 9. 500 mb mean geopotential heights for: from January 1 to March 31, 2020 (a) and February 2020 (b), February 6 2020 (c) and February 11 2020 (d). Maps of temperature anomalies distribution at surface for the Middle East and adjacent areas (K) during, February 6, 2020 (e) and February 11 2020 (f)

Source: data provided by NOAA Physical Sciences Laboratory 2021

Summary and conclusions

Consistent with previous studies, we presented the relationship between winter weather extreme events over Iraq and polar vortex in our case study of 1st–15th February 2020. This paper provided a general overview of the extremes that occurred during the period 1st–15th February 2020 and how they developed. The first half of February 2020 witnessed two contrasting extreme weather events; the first is warm extreme temperature reached its maximum on February 7, when the minimum temperature anomaly was ~ 7 °C in southernmost Iraq. Subsequently, temperatures dropped exceptionally over all Iraq and reached the greatest negative anomaly on February 11 and 12 with temperature anomalies ranging between -6.1°C in the north of Iraq and -10.0°C in the west of Iraq.

The study analyzes the synoptic conditions that made these extreme events among the most severe events in the region during the last four decades.

The study also provides corroborative evidence that the variability in the polar vortex in the lower stratosphere substantially and immediately affects severe winter weather across the Middle East region, and particularly Iraq.

This paper has found that the winter of 2019/20 was marked by a strong and persistent stratospheric north hemisphere polar vortex, associated with significant poleward-moved extratropical cyclone tracks, that led to a remarkably warm and relatively quiet winter across NH mid-latitudes. However, the results also revealed that, with an appropriate polar vortex, a noticeable variability in strength and stability of the polar vortex occurred during the first half of February 2020.

This a short-term change in polar vortex manifested by a sudden variation in westerly circulation around the pole. Moreover, greater values of daily mean eddy heat flux within 45° – 75° N during January and February 2020 were observed on the period 1st to 4th of February that were much higher than the

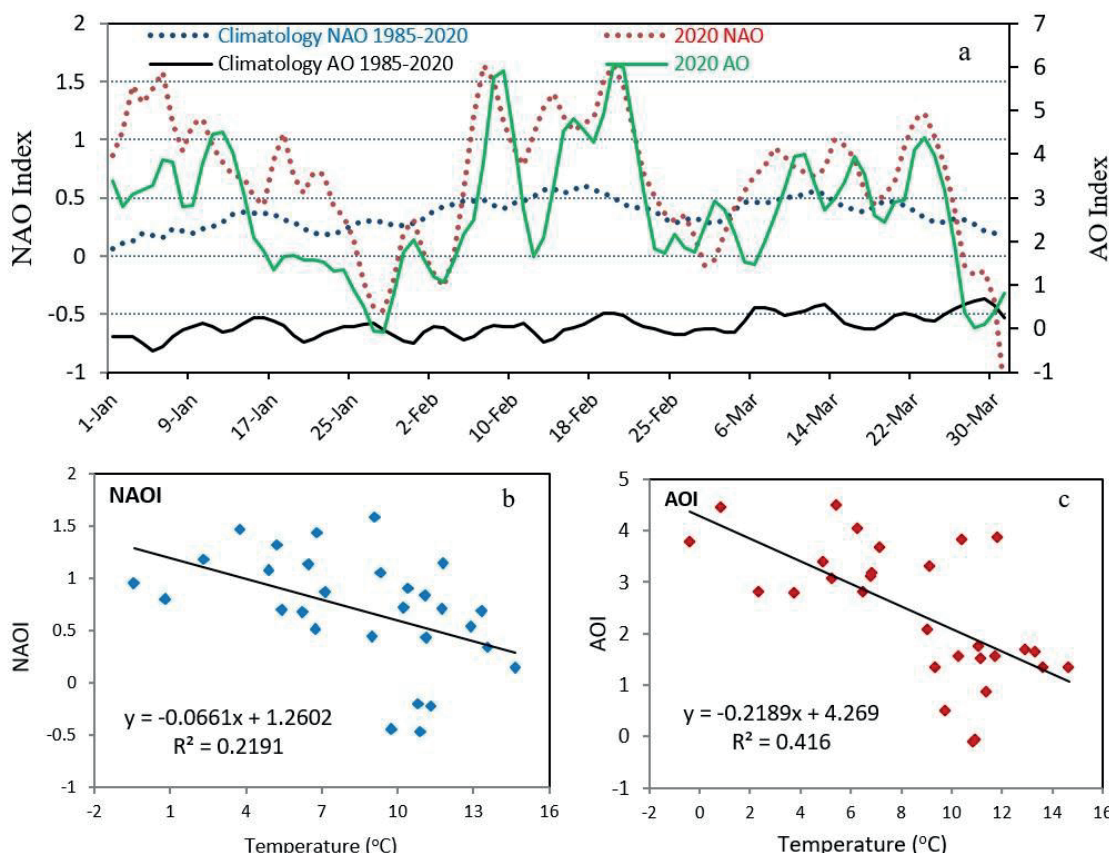


Fig. 10. Daily AO and NAO from January 1, 2020 to March 31, 2020 (a), Scatterplots with correlation between mean daily minimum temperature over Iraq and (the NAOI (b) and AOI (c)), during the period February 1–15, 2020

Source: temperature data from Iraqi Meteorological Organization and Seismology; NAOI and AOI data from NOAA National Centers for Environmental Prediction (NCEP) Climate Prediction Center (CPC)

climatology mean of 1978–2021. The rapid increase in daily mean eddy heat flux means the upward planetary wave activity during the following days was relatively high compared with other days in the 2019/20 winter. The obtained results also identified a significant correlation between some parameters describing polar vortex intensity and daily minimum air temperature over Iraq, particularly with zonal-mean zonal wind at 60° N. This implies that more meridional circulation and extra-frequent cold-air outbreaks occurred over mid-latitudes (including the Middle East region).

Our results show that there are significant changes in the NAO–AO indexes during the end of January through the first half of February. These rapid and short vibrations of the NAO–AO indexes were in response to a change in polar vortex.

Analysis showed that the strong meridional circulation between 45° and 70°N at 100 hPa during the study period led to strengthened ridge and trough systems at 500 hPa. Consequently, this circulation condition enhanced the air exchange between the high and lower latitudes. Around the end of the first week of February, the polar vortex split into two parts, the larger and stronger intensity center was located over North America west of the Greenland Sea. This was deep enough to the substantial northward direction of the polar jet stream over the north-eastern part of the Atlantic sector and western Europe, associated with a large mass of warm air moving to the north Atlantic and eastern Mediterranean region, including Iraq.

Subsequently, the intense polar vortex center gradually moved eastward across the North Atlantic east of Greenland on February 11, leading to a deep trough over the Middle East region. On the surface, an extension of the Siberian anticyclone dominated over the entire eastern Mediterranean region with a central pressure of 1035 hPa. The prevailing synoptic conditions at all atmospheric levels were responsible for the dominance of the extremely cold event associated with heavy snow falling on the early morning of February 11 on most of the northern and central-western parts of Iraq.

Disclosure statement

No potential conflict of interest was reported by the authors.

Author contributions

Study design: KDM; data collection: KDM, AMA; statistical analysis: AMA; result interpretation: KDM; manuscript preparation: KDM, AMA; literature review: AMA.

References

ABDUL RAHMAN MA, 2021, Synoptic analysis of the hail wave and snowfall in Iraq in February 2020. *Al-Adab Journal* 13(1): 249–268. DOI: <https://doi.org/10.31973/aj.v1i139.1396>.

AL-BUDEIRI AL, 2021, Trends in temperature and rain change in Iraq and its future projections. *Al-Adab Journal* 3(137): 443–472. DOI: <https://doi.org/10.31973/aj.v3i137.1129>.

AL-KHALIDI J, DIMA M and STEFAN S, 2018, Large-scale modes impact on Iraq climate variability. *Theoretical and applied climatology* 133: 179–190. DOI: <https://doi.org/10.1007/s00704-017-2180-z>.

AL-QADI TA, MUSLIH KD and SHILTAGH AG, 2021, Analysis of Correlation and Coupling between El Niño-Southern Oscillation and Dust Storms in Iraq from 1971 to 2016. *The Iraqi Geological Journal* 54(1E): 103–113. DOI: <https://doi.org/10.46717/igj.54.1E.9Ms-2021-05-30>.

AL-SAADI MT, 2023, The phenomenon of snowfall in the city of Baghdad using GIS&RS technology. *The American International Journal of Humanities and Social Sciences*. Available at: <https://www.aijhssa.us/>.

AL-TIMIMI YA and AL-KHUDHAIRY A, 2018, Analysis of minimum temperature spatially and temporally over Iraq during the period 1980-2015. *Journal of Applied and Advanced Research* 2: 309–316. DOI: <https://doi.org/10.21839/jaar.2017.v2i5.109>.

AL-TIMIMI YK, AL-LAMI AM, AL-SHAMARTI HA and AL-MAAMORY S, 2020, Analysis of some extreme temperature indices over Iraq. *MAUSAM* 71 (3): 423–430. DOI: <https://doi.org/10.54302/mausam.v7li3.40>.

AMERICAN METEOROLOGICAL SOCIETY, 2015, Polar Vortex. Glossary of Meteorology.

ANGELL JK, 2006, Changes in the 300-mb North Circumpolar Vortex, 1963–2001. *Journal of Climate* 19: 2984–2994. DOI: <https://doi.org/10.1175/JCLI3778.1>.

BALDWIN MP and DUNKERTON TJ, 2001, Stratospheric harbingers of anomalous weather regimes. *Science* 294(5542): 581–584. DOI: [doi/10.1126/science.1063315](https://doi.org/10.1126/science.1063315).

BALDWIN MP, THOMPSON DW, SHUCKBURGH EF, NORTON WA and GILLETT NP, 2003, Weather from the stratosphere? *Science* 30(5631): 317–319. DOI: [10.1126/science.1085688](https://doi.org/10.1126/science.1085688).

BERGHOF FOUNDATION and PEACE PARADIGMS ORGANISATION (PPO), 2023, *Climate change effects on conflict dynamics in Iraq Study of Makhmur, Tal Afar, and Al-Rifai districts*. Berlin: Berghof Foundation Operations.

CELLITTI MP, WALSH JE, RAUBER RM and PORTIS DH, 2006, Extreme cold air outbreaks over the United States, the polar vortex, and the large-scale circulation, *Journal of Geophysical Research (Atmospheres)* 111(D2). DOI: <https://doi.org/10.1029/2005JD006273>.

COHEN J, SCREEN JA, FURTADO JC, BARLOW M, WHITTLESTON D, COUMOU D, FRANCIS J, DETHLOFF K, ENTEKHABI D, OVERLAND J and JONES J, 2014, Recent Arctic amplification and extreme mid-latitude weather. *Nature geoscience* 7: 627–637. DOI: <https://doi.org/10.1038/ngeo2234>.

COUMOU D and RAHMSTORF S, 2012, A decade of weather extremes. *Nature Climate Change* 2(7): 491–496. DOI: <https://doi.org/10.1038/nclimate1452>.

CRAMER W, GUIOT J, FADER M, GARRABOU J, GATTUSO JP, IGLESIAS A, LANGE AM, LIONELLO P, LLASAT MS, PAZ S, PEÑUELAS J, SNOUSSI M, TORETI A, TSIMPLIS MN and XOPLAKI E, 2018, Climate change and interconnected risks to sustainable development in the Mediterranean. *Nature, Climate Change* 8(11): 972–980. DOI: <https://doi.org/10.1038/s41558-018-0299-2>.

ELASHA BO, 2010, *Mapping of climate change threats and human development impacts in the Arab region*. UNDP Arab Development Report–Research Paper Series, Regional Bureau for the Arab States, United Nations Development Programme. New York, United States.

(ESCWA) UNITED NATIONS ECONOMIC AND SOCIAL COMMISSION FOR WESTERN ASIA,

2017, *Arab Climate Change Assessment Report—Main Report*, Beirut.

FINKE K, HANNACHI A and HIROOKA T, 2023, Exceptionally persistent Eurasian cold events and their stratospheric link. *Asia-Pacific Journal of Atmospheric Sciences* 59: 95–111. DOI: <https://doi.org/10.1007/s13143-022-00308-y>.

FRANCIS JA and VAVRUS SJ, 2012, Evidence linking Arctic amplification to extreme weather in mid latitudes. *Geophysical Research Letters* 39(6). DOI: <https://doi.org/10.1029/2012GL051000>.

FRANCIS JA, 2017, Why Are Arctic Linkages to Extreme Weather Still up in the Air? *Bulletin of the American Meteorological Society* 98: 2551–2557. DOI: <https://doi.org/10.1175/BAMS-D-17-0006.1>.

GALYTSKA E, WEIGEL K, HANDORF D, JAISER R, KÖHLER R, RUNGE J and EYRING V, 2023, Evaluating causal Arctic-midlatitude teleconnections in CMIP6. *Journal of Geophysical Research: Atmospheres* 128(17): e2022JD037978. DOI: <https://doi.org/10.1029/2022JD037978>.

HASSAN MW and AL-ASADI KA, 2023, Analysis of large-scale correlations on temperatures over Iraq. *Arab Gulf Journal of Scientific Research* 41(1): 2–17.

HOCHMAN A, MARRA F, MESSORI G, PINTO J G, RAVEH-RUBIN S, YOSEF Y and ZITTIS G, 2022, Extreme weather and societal impacts in the eastern Mediterranean. *Earth System Dynamics* 13(2): 749–777. DOI: <https://doi.org/10.5194/esd-13-749-2022>.

HURRELL JW, 1995, Decadal trends in the North Atlantic Oscillation and relationship to regional temperature and precipitation. *Science* 269: 676–679. DOI: [10.1126/science.269.5224.67](https://doi.org/10.1126/science.269.5224.67).

IPCC, 2023, Climate Change 2023, Synthesis Report. Contribution of Working Groups I, II and III to the Sixth Assessment Report of the Intergovernmental Panel on Climate Change. In: LEE H AND ROMERO J (eds.), IPCC, Geneva, Switzerland. DOI: [10.59327/IPCC/AR6-9789291691647](https://doi.org/10.59327/IPCC/AR6-9789291691647).

IPCC, 2021, Summary for policymakers. In: V. Masson-Delmotte, P. Zhai, A. Pirani, S. L. Connors, C. Péan, S. Berger et al. (Eds.), *Climate change 2021: The physical science basis. Contribution of working group I to the sixth assessment report of the intergovernmental panel on climate change*. Cambridge University Press.

Iraqi Meteorological Organization and Seismology, Department of climate, daily temperature data. (Unpublished data).

KALNAY E, KANAMITSU M, KISTLER R, COLLINS W, DEAVEN D, GANDIN L, IREDELL M, SAHA S, WHITE G, WOOLLEN J, ZHU Y, CHELLIAH M, EBISUZAKI W, HIGGINS W, JANOWIAK J, MO KC, ROPELEWSKI C, WANG J, LEETMAA A, REYNOLDS R, JENNE R and JOSEPH D, 1996, The NCEP/NCAR 40-year reanalysis project. *Bulletin of the American Meteorological Society* 77(3): 437–472. DOI: [https://doi.org/10.1175/15200477\(1996\)077<0437:tnyrp>2.0.co;2](https://doi.org/10.1175/15200477(1996)077<0437:tnyrp>2.0.co;2).

KHIDHER SA and PILESJÖ P, 2015, The effect of the North Atlantic Oscillation on the Iraqi climate 1982–2000. *Theoretical and Applied Climatology* 122: 771–782. DOI: <https://doi.org/10.1007/s00704-014-1327-4>.

KING AD, BUTLER AH, JUCKER M, EARL NO and RUDEVA I, 2019, Observed relationships between sudden stratospheric warmings and European climate extremes. *Journal of Geophysical Research: Atmospheres* 124(13): 943–13 961. DOI: <https://doi.org/10.1029/2019JD030480>.

KÖMÜŞCÜ AÜ and OĞUZ K, 2021, Analysis of cold anomalies observed over Turkey during the 2018/2019 winter in relation to polar vortex and other atmospheric patterns. *Meteorology and Atmospheric Physics* 133: 1327–1354. DOI: <https://doi.org/10.1007/s00703-021-00806-0>.

KURODA Y 2002, Relationship between the polar-night jet oscillation and the annular mode. *Geophysical Research Letters* 29(8): 132–1. DOI: <https://doi.org/10.1029/2001GL013933>.

KUSHNIR Y, DAYAN U, ZIV B, MORIN E and ENZEL Y, 2017, Climate of the Levant: Phenomena and Mechanisms. In: Enzel Y, Bar-Yosef O (eds), *Quaternary of the Levant: Environments, Climate Change, and Humans*. Cambridge University Press.

LAWRENCE Z, PERLWITZ J, BUTLER A, MANNEY G, NEWMAN P, LEE SH and NASH ER, 2020, The remarkably strong arctic stratospheric polar vortex of winter 2020: links to record-breaking arctic oscillation and ozone loss. *JGR Atmos* 125(22): e2020JD033271. DOI: <https://doi.org/10.1029/2020JD033271>.

LEE SH, LAWRENCE ZD, BUTLER AH and KARPECHKO AY, 2020, Seasonal forecasts of the exceptional Northern Hemisphere winter of 2020. *Geophysical Research Letters* 47: e2020GL090328. DOI: <https://doi.org/10.1029/2020GL090328>.

MAHMOUD AY, 2021, The totalitarian situation responsible for snowfall in the city of Baghdad on 11, February 2020. *Al-Adab Journal* 3(139): 221–244. DOI: <https://doi.org/10.31973/aj.v3i139.2291>.

MATTHIAS V and KRETSCHMER M, 2020, The Influence of Stratospheric Wave Reflection on North American Cold Spells. *Monthly Weather Review* 148(4): 1675–1690. DOI: <https://doi.org/10.1175/MWR-D-19-0339.1>.

MedECC, 2020, Climate and Environmental Change in the Mediterranean Basin – Current Situation and Risks for the Future. First Mediterranean Assessment Report. In: Cramer W, Guiot J and Marini K. (eds.), Union for the Mediterranean, Plan Bleu, UNEP/MAP, Marseille, France. DOI: [10.5281/zenodo.4768833](https://doi.org/10.5281/zenodo.4768833).

MOHAMMED A and KADHUM JH, 2021, Dynamical Study for Selective Extreme Events over Iraq and their Relations with General Circulations. *Al-Mustansiriyah Journal of Science* 32(2): 63–70.

MUSLIH KD and BŁAŻEJCZYK K, 2017, The inter-annual variations and the long-term trends of monthly air temperatures in Iraq over the period 1941–2013. *Theoretical and Applied Climatology* 130(1–2): 583–596. DOI: <https://doi.org/10.1007/s00704-016-1915-6>.

MUSLIH KD, 2014, Identifying the climatic conditions in Iraq by tracking down cooling events in the North Atlantic Ocean in the period 3000–0 BC. *Miscellanea Geographica* 18(3): 40–46. DOI: <https://doi.org/10.2478/mgrsd-2014-0016>.

MUTAR ZF and HAMAD NS, 2024, Estimating Long-term Trends in Elements and Some Phenomena of Iraq's Climate. *Dirasat: Human and Social Sciences* 51(5): 33–54. DOI: <https://doi.org/10.35516/hum.v5i5.10018>.

NAQI NM, AL-JIBOORI MH and AL-MADHHACHI AS, 2021, Statistical analysis of extreme weather events in the Diyala River basin, Iraq. *Journal of Water and Climate Change* 12(8): 3770–3785. DOI: <https://doi.org/10.2166/wcc.2021.217>.

NOAA, 2020, National Centers for Environmental Information State of the Climate: Global Climate Report for February 2020, available from NOAA National Centers for Environmental Information State of the Climate.

NOAA National Centers for Environmental Prediction (NCEP) Climate Prediction Center (CPC). Available at: <https://psl.noaa.gov/data/timeseries/daily/list/>.

NOAA Physical Sciences Laboratory 2021, Available at: <https://psl.noaa.gov/data/getpage/>.

Notre Dame Global Adaptation Initiative, “ND-Gain Country Index,” 2022, Available at: <https://gain.nd.edu/our-work/country-index/rankings/>.

OVERLAND J, HALL R, HANNA E, KARPECHKO A, VIHMA T, WANG M and ZHANG X, 2020, The Polar Vortex and Extreme Weather: The Beast from the East in Winter 2018. *Atmosphere* 11(6): 664. DOI: <https://doi.org/10.3390/atmos11060664>.

POLVANI, LM and WAUGH DW, 2004, Upward wave activity flux as a precursor to extreme stratospheric events and subsequent anomalous surface weather regimes. *Journal of Climate* 17(8): 3548–3554. DOI: [https://doi.org/10.1175/1520-0442\(2004\)017<3548:UWAFAA>2.0.CO;2](https://doi.org/10.1175/1520-0442(2004)017<3548:UWAFAA>2.0.CO;2).

RAHIMI N, 2021, Analyzing the Role of Polar Vortex on Daily Extreme Precipitation in the Northwest of Iran. *Geography and Environmental Sustainability* 11(4): 59–82.

RODGERS JL and NICEWANDER WA, 1988. Thirteen ways to look at the correlation coefficient. *The American Statistician* 42(1): 59–66.

SALMAN SA, SHAHID S, ISMAIL T, CHUNG ES and AL-ABADI AM, 2017, Long-term trends in daily temperature extremes in Iraq. *Atmospheric research* 198: 97–107. DOI: <https://doi.org/10.1016/j.atmosres.2017.08.011>.

SCHOEBERL MR and HARTMANN DL, 1991, The dynamics of the stratospheric polar vortex and its relation to springtime ozone depletions. *Science* 251: 46–52.

SCREEN JA, DESER C, SMITH DM, ZHANG X, BLACKPORT R, KUSHNER PJ, QUDAR T, MCCUSKER KE and SUN L, 2018, Consistency and discrepancy in the atmospheric response to arctic sea-ice loss across climate models. *Nature Geoscience* 11(3): 155–163. DOI: <https://doi.org/10.1038/s41561-018-0059-y>.

SENEVIRATNE SI, ZHANG X, ADNAN M, BADI W, DERECZYNSKI C, DI LUCA A, GHOSH S, ISKANDAR I, KOSSIN J, LEWIS S and OTTO F, 2021, *Weather and climate extreme events in a changing climate. Climate Change 2021: The Physical Science Basis. Contribution of Working Group I to the Sixth Assessment Report of the Intergovernmental Panel on Climate Change*. Cambridge, UK & New York USA.

THOMPSON DWJ and WALLACE JM, 1998, The Arctic oscillation signature in the wintertime geopotential height and temperature fields. *Geophysical research letters* 25(9): 1297–1300.

WALLACE JM and GUTZLER DS, 1981, Teleconnections in the geopotential height field during the Northern Hemisphere winter. *Monthly weather review* 109: 784– 812.

WAUGH DW, SOBEL AH and POLVANI LM, 2017, What is the polar vortex and how does it influence weather? *Bulletin of the American Meteorological Society* 98: 37–44. DOI: <https://doi.org/10.1175/BAMS-D-15-00212.1>.

WEGMANN M, ORSOLINI Y, VAZQUEZ M, GIMENO L, NIETO R, BULYGINA O, JAISER R, HANDORF D, RINKE A, DETHLOFF K, STERIN A and BRÖNNIMANN S, 2015, Arctic moisture source for Eurasian snow cover variations in autumn. *Environmental Research Letters* 10(5): 054015.

ZHANG J, SHENG Z, MA Y, HE Y, ZUO X and HE M, 2021a, Analysis of the Positive Arctic Oscillation Index Event and Its Influence in the winter and spring of 2019/2020. *Frontiers in Earth Science* 8: 580601.

ZHANG XD, FU YF, GUAN ZY, TANG H, WANG GM, WANG ZM, WU PL and YANG XQ, 2020, Influence of Arctic warming amplification on Eurasian winter extreme weather and climate: Consensus, open questions, and debates. *Journal of the Meteorological Sciences* 40: 596–604. DOI: <https://doi.org/10.1016/j.atmosres.2023.107030>.

ZHANG Y, CAI Z and LIU Y, 2021b, The exceptionally strong and persistent Arctic stratospheric polar vortex in the winter of 2019–2020. *Atmospheric and Oceanic Science Letters* 14(2): 100035.

ZITTIS G, ALMAZROUI M, ALPERT P, CIAIS P, CRAMER W, DAHDAL Y & LELIEVELD J, 2022, Climate change and weather extremes in the Eastern Mediterranean and Middle East. *Reviews of Geophysics* 60(3): e2021RG000762. DOI: <https://doi.org/10.1029/2021RG000762>.

Received 28 September 2024

Accepted 19 January 2025